Convergent Evolution of Broadband Reflectors Underlies Metallic Coloration in Butterflies

Anna Ren[1†], Christopher R. Day[1,2†], Joseph J. Hanly[1], Brian A. Counterman[3], Nathan I. Morehouse[4] and Arnaud Martin[1]*

[1] Department of Biological Sciences, The George Washington University, Washington, DC, United States, [2] Epigenetics and Stem Cell Biology Laboratory, National Institute of Environmental Health Sciences, National Institutes of Health, Durham, NC, United States, [3] Department of Biological Sciences, Mississippi State University, Starkville, MS, United States, [4] Department of Biological Sciences, University of Cincinnati, Cincinnati, OH, United States

Butterfly wings often display structural colors, which are the result of light reflection from chitinous nanostructures that adorn the wing scales. Amongst these structural colors are broadband metallic reflections, which have been previously linked to an ultrathin broadband reflector in the nymphalid butterfly *Argyrophorus argenteus*. To test if similar optical modes of broadband, specular reflectance have evolved in other butterfly taxa, we characterized the reflective scales of eight species from five Papilionoidea families using microspectrophotometry (MSP), light microscopy in reflected and transmitted modes, and scanning electron microscopy (SEM). In Nymphalidae, Pieridae, and Hesperidae, and Lycaenidae, we find that broadband specularity is due to spatial mixing of densely juxtaposed colorful reflectances that change across microscale distances (e.g., 1–3 μm). These seemingly convergent silver scales are unpigmented, show a continuous upper lamina with reduced windows, and consist of an air-cuticle sandwich of variable thickness, forming an undulatory thin-film. Strikingly, *Hypochrysops apelles* (Lycaenidae) shows a novel mode of silver reflectance with spatial color mixing occurring across the entire proximo-distal length of the scale (>100 μm), transitioning from blue to red hues between the stem and the tip of the scales. Unlike the undulatory type, this reflector shows flat thin-films which also includes a multilayered lower lamina, responsible for selective color iridescence in other lycaenids or in sunset moths. Finally, the gold scales of *Anteros formosus* (Riodinidae) show mixed reflectance in the green-to-red range, seemingly produced by a thin film in the lower lamina. Our comparative study suggests that evolution of metallic broadband reflectance repeatedly involved spatial color mixing and unperforated upper laminae, and is accomplished using at least three types of ultrastructural modifications. Undulatory thin-film systems, based on geometric adjustments of the transverse profile of the upper lamina and scale lumen, are widespread and may have evolved repeatedly from more generic colorless scale morphologies, while lycaenid and riodinid broadband reflectors may be elaborations of pre-existing iridescent states.

Keywords: structural colors, specular reflectance, Lepidoptera, convergent evolution, cuticular ultrastructure

INTRODUCTION

Biological mirrors and tissues with metallic appearances have evolved in many forms across the tree of life (Land, 1972) – from fish skin (McKenzie et al., 1995; Levy-Lior et al., 2008; Jordan et al., 2012), to scarab beetles (Agez et al., 2017), squid eyes (Holt et al., 2011; Ghoshal et al., 2013), and even begonia leaves (Lee, 2009; Zhang et al., 2009). Rather than relying on pigments *per se*, these mirror-like tissue reflectances result from microscopic optical structures that backscatter a wide spectrum of continuous wavelengths. For instance, dermal layers of guanine crystals of random thickness and distribution form a disordered stack termed a chaotic reflector and generate the broadband reflectance that gives herring and sardines their silvery aspect (Denton and Land, 1971; Levy-Lior et al., 2008; Jordan et al., 2012). Metallic reflections are also common among arthropods, including the elytra of many species of beetles and the pupal casing of some butterflies (Neville, 1977; Steinbrecht et al., 1985; Berthier, 2007; Kinoshita, 2008; Biro and Vigneron, 2011; Agez et al., 2017). These examples of insect metallic colors rely on broadband reflectance from multiple layers of chitin with differing thicknesses, often termed chirped stacks (Kinoshita and Yoshioka, 2005; Biro and Vigneron, 2011). As in the chaotic reflector, those chirped mirrors are often hundreds of microns thick because they rely on the stacking of bilayers of dielectric materials with distinctive refractive indices (Deparis et al., 2006; Cook and Amir, 2016; Chiadini et al., 2017), typically from air or cytoplasm (low-index $1 < n_L < 1.33$), and chitin (high-index $1.53 < n_H < 1.56$), melanized chitin (high-index $1.56 < n_H < 1.8$), or guanine platelets ($1.46 < n_H < 1.85$) (Leertouwer et al., 2011; Jordan et al., 2012; Stavenga et al., 2015a). Reducing the thickness of a chirped mirror theoretically requires increasing the number and refractive index of the dielectric materials. In particular, the difference in refractive index between layers determines how much light is reflected at each interface. The smaller this difference, the less light is reflected, implying that chirped stacks relying on natural materials can only achieve reasonable reflectances using multilayers of 10 thin films or more (Land, 1972; Cook and Amir, 2016).

The wing scales of butterflies and moths (order: Lepidoptera) are typically 1–2 μm thick. In contrast with thick chirped and chaotic reflectors, they have evolved *ultrathin* broadband reflectors only requiring sub-micron thickness (Vukusic et al., 2008; Stavenga et al., 2012; Wilts et al., 2013), often by the mixing of colors across a reflective surface rather than producing broadband reflectance at all points on the surface as in chirped stacks. In the examples described to date, broad spectrum reflectance of the wing scales results from the spatial mixing of parallel strips of colors that run alongside the periodic ridges of the reflective scale side (Vukusic et al., 2008), and derive from thin-film interference between air and two chitin layers, called the lower and upper laminae. The color heterogeneity is produced by an undulatory thin-film interface, where the sawtooth-shaped cross-sectional profile of the scale and the varying thicknesses of the air layer result in the reflection of a wide range of colors across a single scale. Such color variation disappears from the far field scattering appearance of these scales, where spatial mixing results in an overall broadband reflectance (Vukusic et al., 2008; Stavenga et al., 2012; Wilts et al., 2013).

Metallic reflectances are widespread across the Lepidoptera, suggesting that the morphologies underlying them may be relatively "accessible" in the evolutionary sense (e.g., achievable by simple changes to scale architecture). There are a number of ways that such transitions to metallic coloration might occur. The current literature provides a limited view of the broader evolutionary patterns of metallic coloration in butterflies. Prior studies indicate that silvery states may have evolved at least three times, in Hesperiidae (Ge et al., 2017), Nymphalidae (Vukusic et al., 2008), and Lycaenidae (Wilts et al., 2013), presumably via relatively simple departures from the traditional scale architecture to achieve the mechanism described above (Ghiradella, 2010). Those cases invariably display a highly reflective configuration under the form of ectopic lamination, i.e., an apparent covering of the micropores (sometimes called *windows* or *pepper-pots*) that perforate the upper lamina of less reflective scales. This kind of simplification of the upper lamina to a film-like sheet has been consistently observed in scanning electron micrographs of silver-metallic scales, including from nymphalid species of the Heliconiinae and Satyrinae sub-families (Simonsen, 2007; Giraldo, 2008; Vukusic et al., 2008; García-Barros and Meneguz, 2012; Dinwiddie et al., 2014), in the lycaenid *Curetis acuta* (Wilts et al., 2013; Liu et al., 2019), and in the hesperid *Carystoides escalantei* (Ge et al., 2017). In the polymorphic species *Argynnis niobe,* scales from flat white spots show more perforation of the upper lamina compared to scales from individuals with brighter, recognizably silver spots (Simonsen, 2007). Thus, silver scales could be a more reflective elaboration of white scales, perhaps by reduction of the upper lamina fenestration.

Alternatively, broad-spectrum reflectance could evolve from increased disorder in iridescent scales that are already highly reflective, i.e., iridescent scale types with a more narrow color profile. Referring to a classification of mechanisms of iridescence in butterflies (Ghiradella, 1989; Vukusic et al., 2000; Mouchet and Vukusic, 2018), silver scales could derive from "Type II" body-lamellae scales, especially the Type IIa scales (or *Urania*-type) that are the most common mode of iridescence in Lycaenidae (Lippert and Gentil, 1959; Schmidt and Paulus, 1970; Tilley et al., 2002; Biró et al., 2007). Unlike silver scales, Type IIa scales generate iridescent colors by internal multilayering (Ghiradella, 1989; Wilts et al., 2008; Yoshioka et al., 2013), and show a level of reflectance that is linearly proportional to the extent of upper lamina filling (Wilts et al., 2008). Whether this configuration can yield the spatial color mixing of heterogeneous colors and achieve broad reflectance spectra remains an open question. Finally, none of the previously profiled silver scale architectures shows "Type I" ridge-lamellae scales emblematic of blue *Morpho* butterflies, or "Type III" body-scattering structures that involve a porous upper lamina opening into crystal-like inclusions such as pigment granules or gyroid structures (Vukusic et al., 2000; Dolan et al., 2015; Singer et al., 2016; Wilts et al., 2017; Mouchet and Vukusic, 2018). We shall note, however, that there are no reported studies

of metallic coloration and its underlying structural causes in either the Pieridae or the Riodinidae, which is surprising in the latter case given the family's vernacular name of "metalmarks." The mechanisms of broadband reflectance in those clades thus remain unexplored.

In this study we sought to expand our comparative knowledge of the ultrastructures underlying specular (mirror-like), broad-spectrum reflectance in butterflies, or in other words, to explore the diversity of scales showing metallic coloration. Using a combination of transmitted and reflected light microscopy, electron microscopy, and microspectrophotometry, we describe the modalities of specular, broad-spectrum reflectance and derive insights into the convergent evolution of metallic colors across butterflies.

RESULTS

Silver Coloration Exists in Five Out of Seven Butterfly Families

To gain insights into the diversity of structures underlying metallic broadband reflectance in the wing scales of butterflies (superfamily Papilionoidea), we selected one or two representatives from five of the seven families in this lineage (**Figure 1A**): Nymphalidae (*Agraulis vanillae* and *Speyeria cybele*, sub-family: Heliconiinae), Lycaenidae (*Hypochrysops apelles*, sub-family: Theclinae and *Cigaritis lohita*, sub-family: Aphnaeinae), Riodinidae (*Anteros formosus*, sub-family: Riodininae), Pieridae (*Colias eurytheme* and *Zerene cesonia*, sub-family: Coliadinae), and Hesperidae (*Epargyreus clarus*, sub-family: Eudaminae). We found no clear case of silver reflectance in the Hedylidae family, which includes only one extant genus. We also omitted Papilionidae, though it is noteworthy that certain morphs of the endangered species *Baronia brevicornis brevicornis* display silver patches with bright reflectance (Vazquez, 1987), and that broad-spectrum light-scattering scales with a diffuse white appearance have been described in *Graphium sarpedon* (Stavenga et al., 2010, 2012).

While the gold/silver metallic color elements of our specimens were always on the ventral side, this may be a trend rather than a rule, as illustrated by the nymphalid *Argyrophorus argenteus* that displays a completely silver dorsal side (Vukusic et al., 2008). Overall, this phylogenetic sampling may represent at least four cases of homoplasy, with at least one origin in each of the nymphalid, lycaenid and riodinid, pierid, and hesperid lineages, or more independent acquisitions of the specular, broad-spectrum reflectance. In contrast, we can assume a likely homology between silver scales found in the ventral hindwing silver blotches from "fritillary butterflies" of the Heliconiinae sub-family (here, *A. vanillae* and *S. cybele*), or in the ventral discal ocelli of Coliadinae (*C. eurytheme* and *Z. cesonia*); we thus sampled two species in each lineage to get insights on the range of divergence within silver scales of shared origin and context. The reflectance of all silver elements extended into the ultraviolet range, as shown by UV-photography excluding visible light wavelengths above 400 nm (**Figure 1B**).

Metallic Scales Are Unpigmented, Except in Lycaenidae and Riodinidae

We isolated single scales from metallic elements of the eight sampled species for further observations, with all subsequent images and analyses focused on silver elements from the hindwings (**Figure 1C**). In order to assess the relative contribution of pigmentation and structural thin-film interference to silver scale coloration, we used reflected-light microscopy in air (refractive index $n = 1$) and transmitted-light microscopy under clove oil immersion ($n = 1.53$), a medium that matches the refractive index of chitin and thus substantially reduces light diffraction (Mayor, 1806; Stavenga et al., 2015b; Thayer et al., 2020). When immersed in clove oil, silver scales from species belonging to Nymphalidae, Pieridae, and Hesperiidae turned transparent, highlighting a lack of pigment (**Figures 1D,E**). In contrast, the metallic scales of the three lycaenid and riodinid species showed a small amount of light-brown pigmentation, likely melanin, which increases the refractive index of chitin and may thus change the reflectance of the scale (Land, 1972).

Metallic Scales Show Consistent Modifications of Their Upper Surfaces

We examined the exterior features of silver scales in scanning electron micrographs, and systematically compared them to adjacent non-reflective scale types. As in previous studies (see section "Introduction"), metallic scales showed extensive lamination, where the spaces between crossribs are filled rather than left empty, as found in less reflective scales (**Figure 2**). With the exception of the closely related *Z. cesonia* and *C. eurytheme*, all silver scales also showed an increase in inter-ridge distance (**Figures 3A,C**). Increasing the surface of light-reflecting upper laminae could be of functional importance, particularly in the two species where inter-ridge spacings are the most differentiated: silver scale ridge intervals are $1.5\times$ larger than in adjacent scales in *A. vanillae* (silver, mean = 2.29 μm; black, mean = 1.45 μm), and $2.4\times$ larger in *H. apelles* (silver, mean = 2.73 μm; orange, mean = 1.16 μm). Finally, all silver scales were wider than adjacent scales (**Figures 3B,D**), indicating that silver scales may be tuned to provide dense coverage on the wing and maximize the surface area of light reflectance. Thus, compared to light-absorbing, pigment-colored scales, metallic scales achieve higher reflectance by maximizing the opportunity for backscattering of incident light via three concomitant mechanisms: expansion of lamination/decrease in fenestration of upper wing scale surface, increase in ridge distance, and increase in overall scale width. In the next section, we investigate possible mechanisms underlying the broad spectrum reflectance of these specialized scales.

Undulatory Thin-Film Broadband Reflectors Are Widespread

In order to substantiate the broad reflectance of silver scales that can be inferred from direct observation and UV-photography, we used a microspectrophotometer to compare the reflectance spectra of metallic scales *vs.* adjacent, non-metallic scales from each species (**Figures 4A–E**). We focus on nymphalid, pierid, and
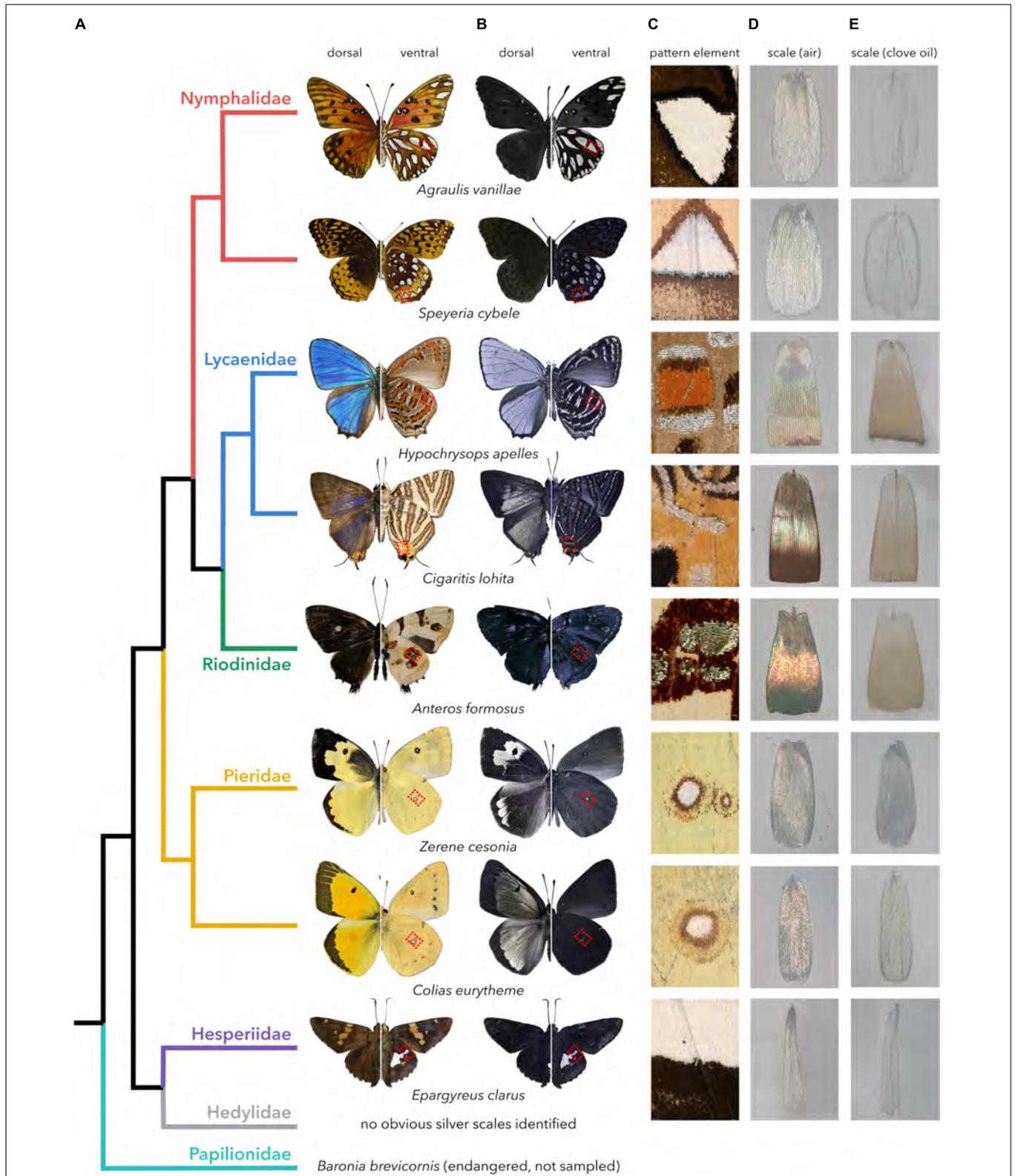
FIGURE 1 | Repeated occurrence of metallic scales in butterflies. **(A)** Phylogenetic relationships between the eight species sampled in this study (Espeland et al., 2018; Wiemers et al., 2019). **(B)** Ultraviolet (UV-B) photographs reveal reflectance in the non-visible range. **(C)** Magnified views of the reflective patterns obtained by a digital microscope, corresponding to red square insets in panels **(A,B)**. **(D,E)** Reflected-light microscopy of single silver or gold scales in air ($n = 1$) and transmitted-light in clove oil ($n = 1.53$).

FIGURE 2 | Modified morphologies of metallic scales in five butterfly families. (A,B) Nymphalidae. (C,D) Pieridae. (E,F) Lycaenidae. (G) Riodinidae. (H) Hesperiidae. Each panel shows a silver pattern imaged by digital light microscopy (left insets, scale bars = 100 μm), and close-up views of non-metallic (upper rows) vs. metallic (lo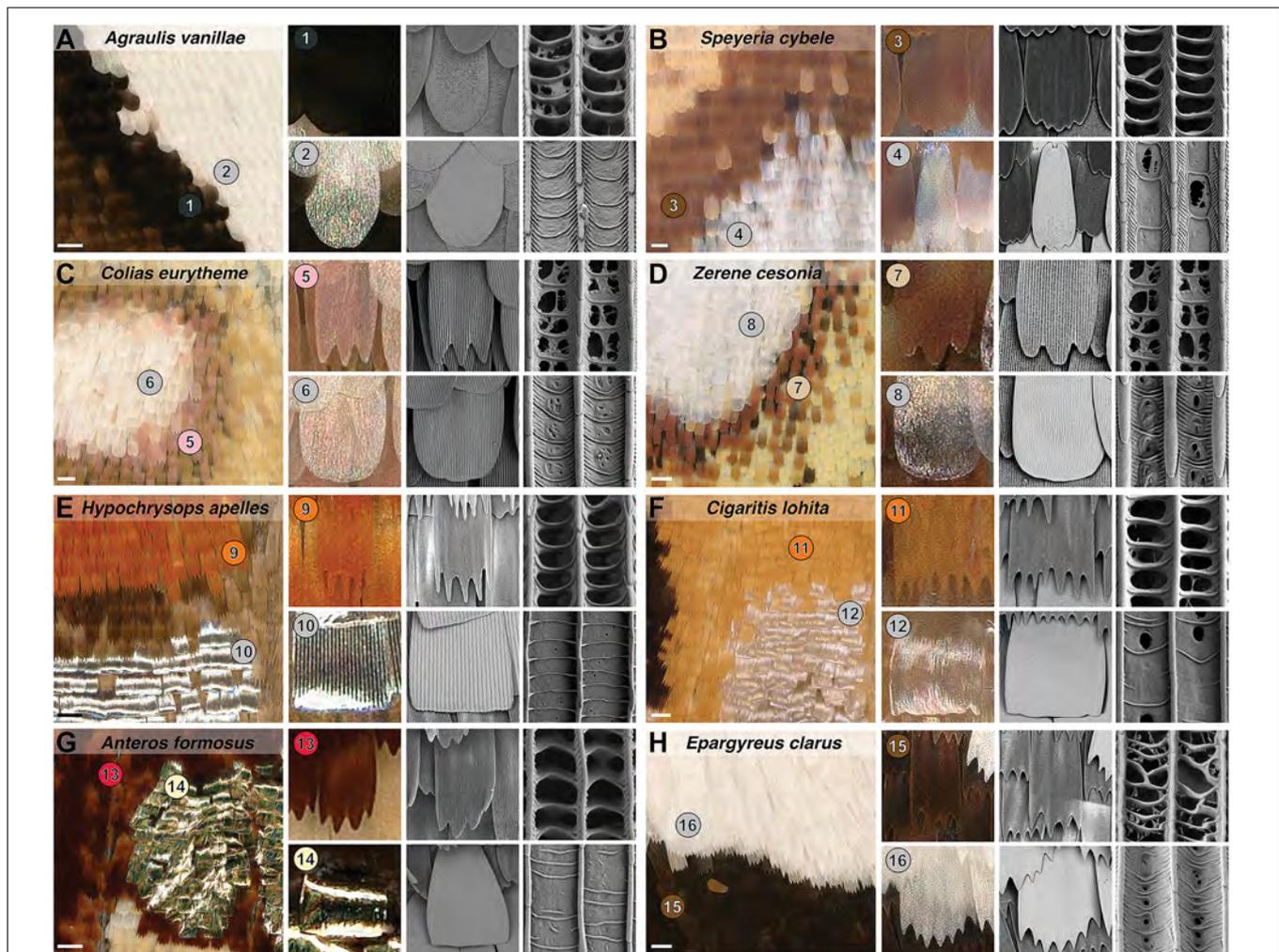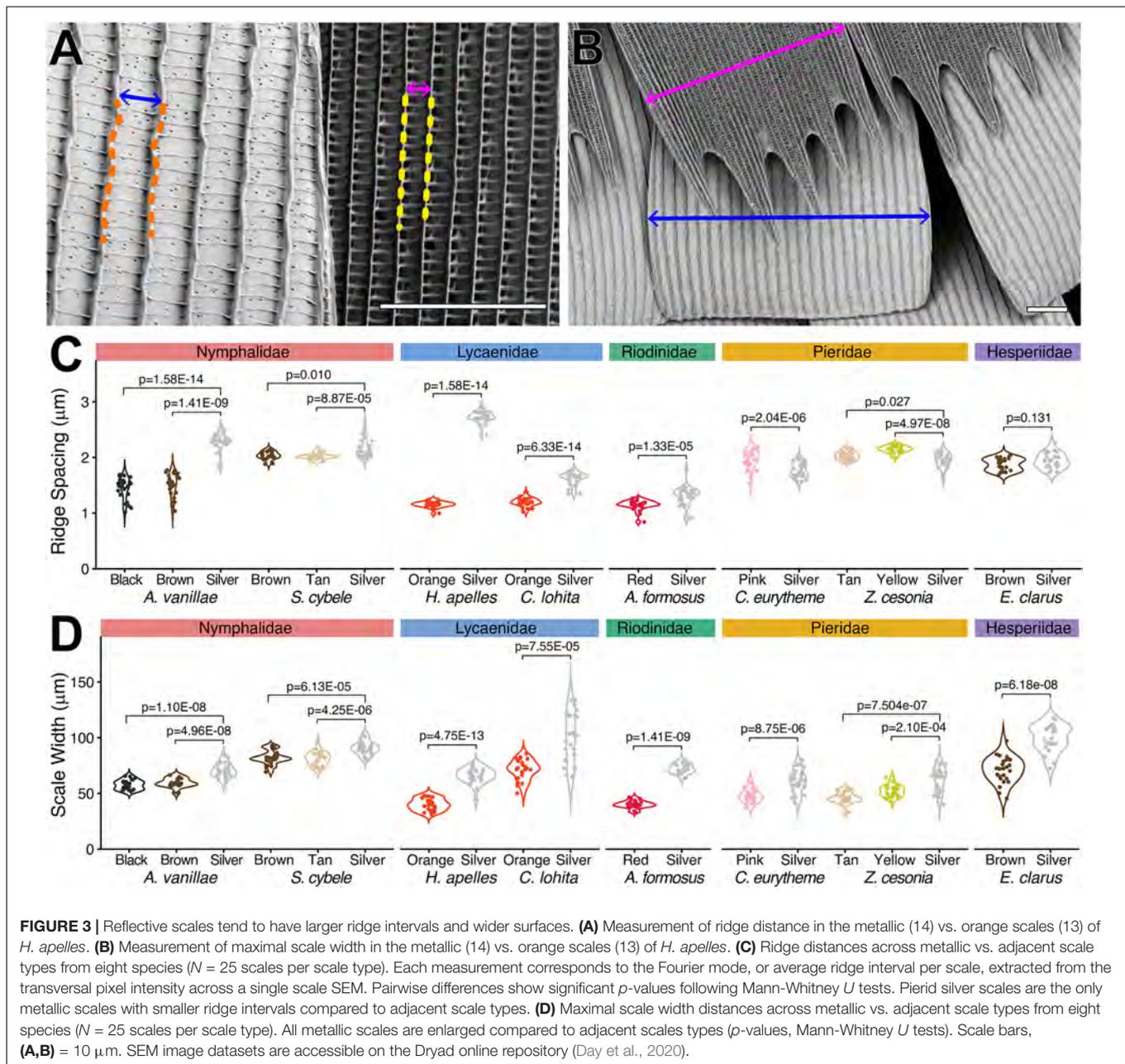wer rows) scales under light and electron microscopy. The right columns show the ultrastructural details of the upper lamina, highlighting the fenestration of non-metallic scales vs. the smooth surface of reflective scales across two inter-ridge intervals. Numbered bullets mark scale types and species that are referred to in further figures.

hesperid samples first, and will address the more unusual optical morphologies observed in the lycaenid/riodinid clade samples in subsequent sections.

The unpigmented silver scales of *A. vanillae* and *S. cybele* (sub-family: Heliconiinae) produced a relatively flat reflectance spectra across the UV and visible range (300–700 nm) and extending into the infrared range (700–800 nm), consistent with previous results (Briscoe et al., 2010). Hesperid (*E. clarus*) and pierid (*C. eurytheme*, *Z. cesonia*) unpigmented scales showed a similar broad reflectance. The discal spot scales of *Z. cesonia* reflected less than half of the light reflected by laboratory-grade aluminum foil (**Figures 4E,F**), which is used here as a familiar point of comparison. Finally, all measurements of reflective surfaces showed more variation across measurements compared to adjacent pigmented scales, due to surface irregularities and the angle-dependency of light reflectance in the silver samples.

Next, we used reflected-light microscopy to test if those unpigmented silver scales would reproduce the pattern of spatial color mixing previously described in *A. argenteus* (sub-family: Satyrinae). In this species, color strips run parallel to the scale ridges as the sawtooth profile of the upper lamina imposes variation in the thickness of the subjacent air lumen (Vukusic et al., 2008; Mouchet and Vukusic, 2018). This ultrathin configuration produces dense rods of colors, each less than 1–3 μm thick, that alternate across the scale width. We found that similar stripes can be discerned in *A. vanillae* and *S. cybele* (**Figures 4G,H**), while in *E. clarus*, *Z. cesonia*, and *C. eurytheme*, individual colors are more speckled and pointillist (**Figures 4I–L**). Thus, all five species from the Nymphalidae, Pieridae, and Hesperiidae achieve broad-spectrum reflectance via dense spatial color mixing spread across the scale surface.

FIGURE 3 | Reflective scales tend to have larger ridge intervals and wider surfaces. **(A)** Measurement of ridge distance in the metallic (14) vs. orange scales (13) of *H. apelles*. **(B)** Measurement of maximal scale width in the metallic (14) vs. orange scales (13) of *H. apelles*. **(C)** Ridge distances across metallic vs. adjacent scale types from eight species (*N* = 25 scales per scale type). Each measurement corresponds to the Fourier mode, or average ridge interval per scale, extracted from the transversal pixel intensity across a single scale SEM. Pairwise differences show significant *p*-values following Mann-Whitney *U* tests. Pierid silver scales are the only metallic scales with smaller ridge intervals compared to adjacent scale types. **(D)** Maximal scale width distances across metallic vs. adjacent scale types from eight species (*N* = 25 scales per scale type). All metallic scales are enlarged compared to adjacent scales types (*p*-values, Mann-Whitney *U* tests). Scale bars, **(A,B)** = 10 µm. SEM image datasets are accessible on the Dryad online repository (Day et al., 2020).

Based on those observations, we hypothesized that these metallic scales would resemble the bilayered internal anatomy of *A. argenteus* scales, and examined the SEM profile of those scale samples after transversal cryofracture (**Figure 5**). We found that *A. vanillae*, *E. clarus*, *C. eurytheme*, and *Z. cesonia* share the serrated profile of *A. argenteus*, characterized by two laminae of relatively constant thickness and an internal air layer of varying thickness ("undulatory lumen"). *S. cybele* likewise has an undulating profile in its upper section, but with a flat lumen and an upper lamina of varied thickness that resembles "speed bumps," due to local chitin thickening of the ridge area (**Figure 5B**). Of note, under near-field observation, *S. cybele* shows a single strip of color per ridge interval of 2–2.3 µm

(**Figure 5H'**), while in other nymphalids such as *A. vanillae* (**Figure 5G'**) and *A. argenteus* (Vukusic et al., 2008), multiple color transitions can be observed within a single ridge interval of comparable dimensions (**Figure 3B**). Thus, the *S. cybele* mode of undulation is structurally distinct from other examples (**Figure 5F**), and achieves similar broadband reflectance albeit through a coarser mode of spatial color mixing.

Nonetheless, the similarities between these morphologies suggest that the optical principles of an undulatory thin-film reflector are at play across these butterfly lineages, with wavelength-specific variation in light reflectance across the scale surface due to the periodic profiles of either the upper chitin layer or the scale lumen. We suggest the previous biophysical

FIGURE 4 | Silver broadband reflectance resulting from densely intermixed colored reflections. **(A–E)** Reflectance spectra of silver pattern elements (gray lines), compared to adjacent arrays of non-reflective scales (black, brown, pink and beige lines). Faded lines represent individual measurements taken within the same wing surface. Dotted lines indicate the averaged spectra of polished aluminum foil for comparison. **(F)** Reflectance spectra of the polished side (gray) and dull side (blue) of aluminum foil. **(G–K')** High-magnification reflected-light microscopy of single silver scales using a MPlanFLN 50× lens **(G–K)**, and an LMPlan Achromatic 100× lens **(G'–K')**. **(L,L')** High magnification reflected light microscopy of dull and polished sides of aluminum foil under the 100× lens. Scale bars: **(G–K)** = 20 μm; **(G'–K',L,L')** = 10 μm.

characterization of a butterfly undulatory thin-film reflector (Vukusic et al., 2008) applies here, and infer that this general mechanism accounts for multiple cases of metallic iridescence in Nymphalidae, Hesperiidae, and Pieridae. Such reflectors may have evolved repeatedly by tuning pre-existing scale elements of the scale groundplan (Ghiradella, 2010) to create a undulatory
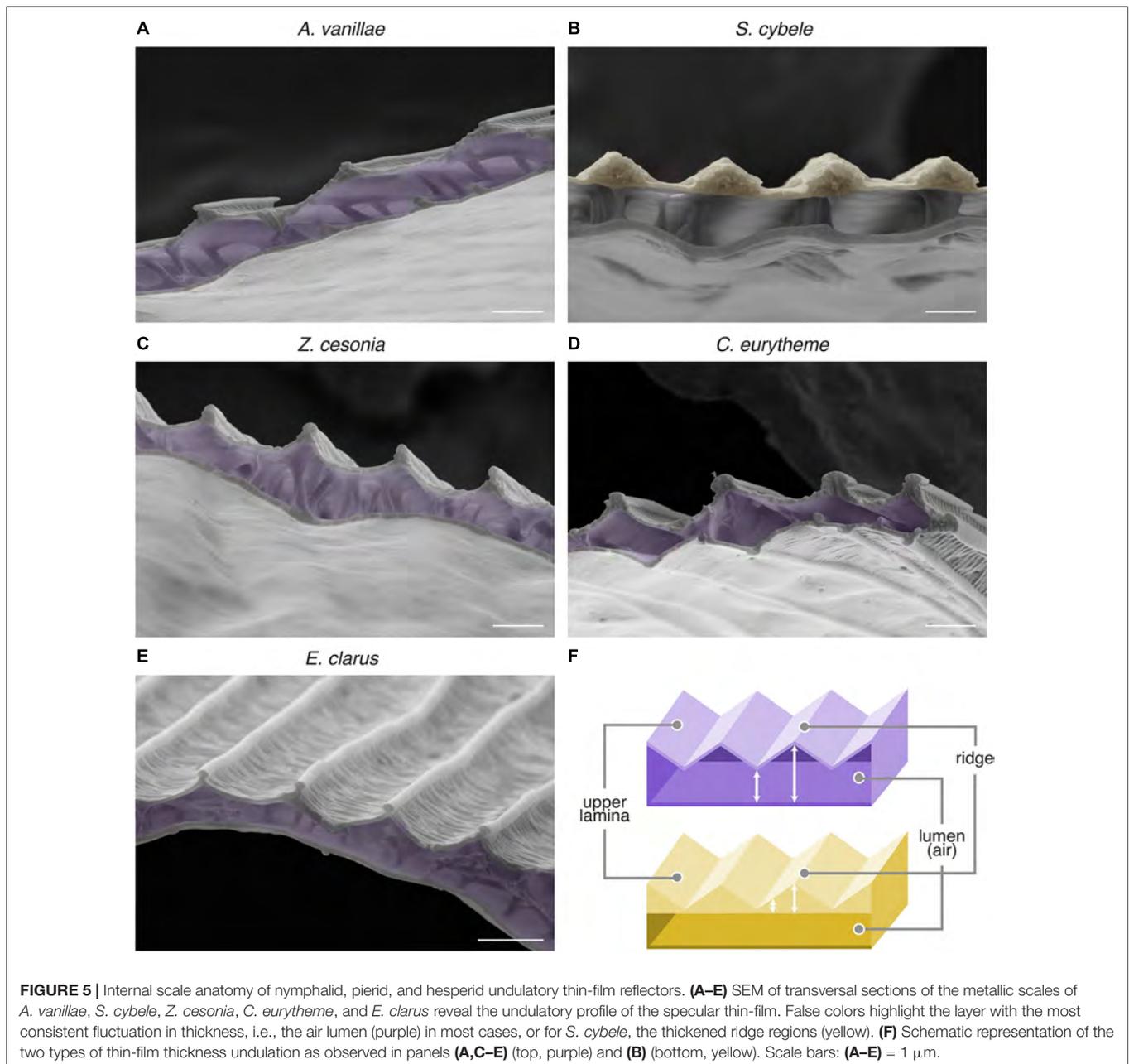
FIGURE 5 | Internal scale anatomy of nymphalid, pierid, and hesperid undulatory thin-film reflectors. **(A–E)** SEM of transversal sections of the metallic scales of *A. vanillae*, *S. cybele*, *Z. cesonia*, *C. eurytheme*, and *E. clarus* reveal the undulatory profile of the specular thin-film. False colors highlight the layer with the most consistent fluctuation in thickness, i.e., the air lumen (purple) in most cases, or for *S. cybele*, the thickened ridge regions (yellow). **(F)** Schematic representation of the two types of thin-film thickness undulation as observed in panels **(A,C–E)** (top, purple) and **(B)** (bottom, yellow). Scale bars: **(A–E)** = 1 μm.
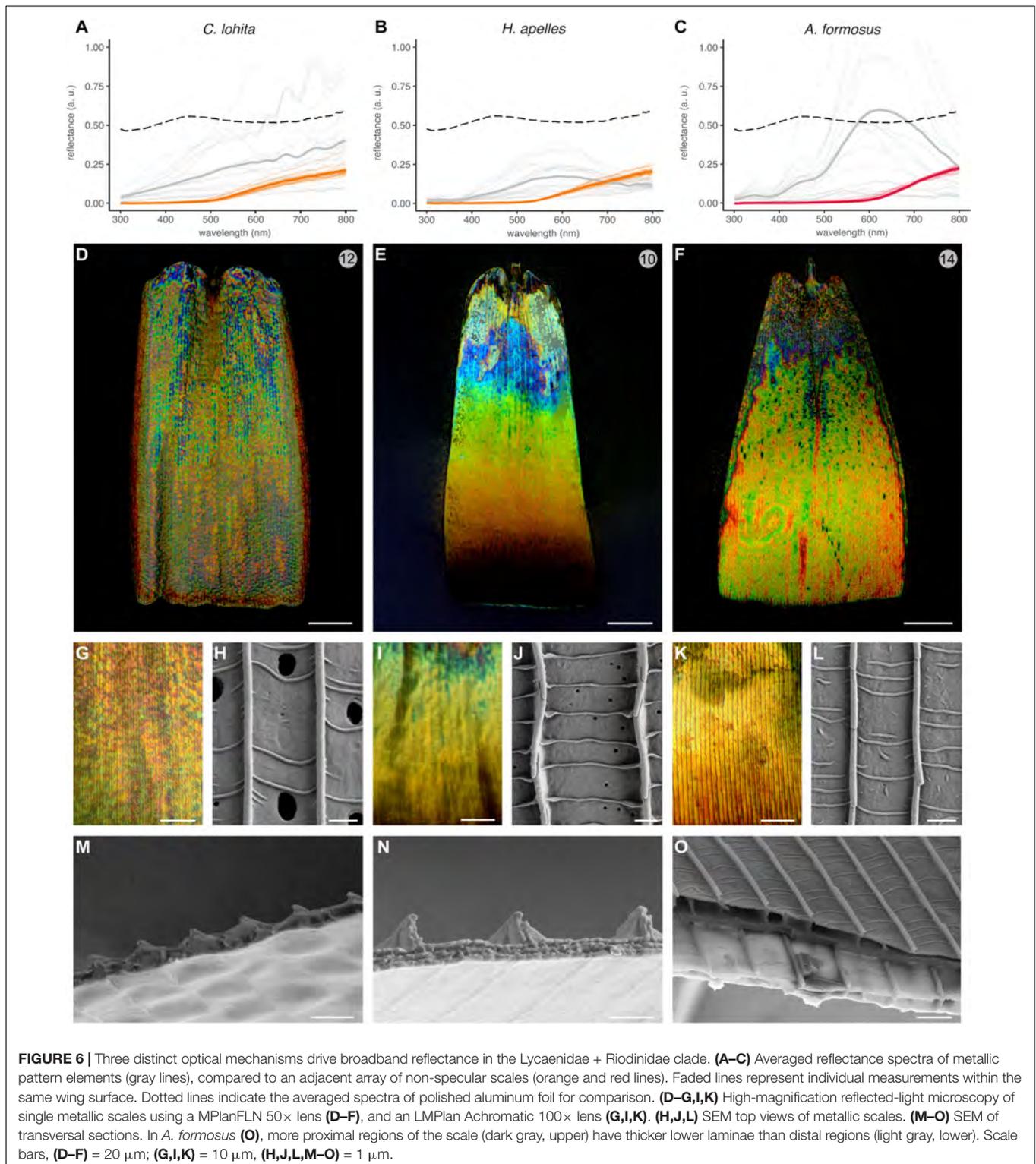
thin-film system with a single inner air layer between the upper and lower laminae.

Two Modes of Broadband Reflectance in Lycaenidae

We also examined the features of silver scales from *C. lohita* and *H. apelles,* two lycaenid species, and from the gold scales of *A. formosus*, a species from the riodinid sister lineage (**Figure 6**). All three types of metallic scales differed from other sub-families. The silver scales of *C. lohita* showed optical and structural features reminiscent of the undulatory thin-film configuration found in Nymphalidae, Hesperiidae, and Pieridae in this study,

as well as in the specular scales of *Curetis acuta*, another lycaenid (Wilts et al., 2013; Liu et al., 2019). In particular the reflectance spectra, color speckling at microscopic levels, upper lamina external views, and transversal inner anatomies all resembled the hesperid and pierid samples (**Figures 6A,D,G,H,M**). Thus, the *C. lohita* reflector follows an undulatory thin-film architecture, providing yet another evolutionary occurrence of this category of mechanism in a fourth butterfly family.

In contrast, the silver scales of *H. apelles* showed a distinctive spectrum and a strikingly divergent mode of color mixing, with a continuous color transition, from blue to red, stemming from the base to the distal region of the scale (**Figures 6B,E,I**). This longitudinal gradient represents a novel, previously undescribed

FIGURE 6 | Three distinct optical mechanisms drive broadband reflectance in the Lycaenidae + Riodinidae clade. **(A–C)** Averaged reflectance spectra of metallic pattern elements (gray lines), compared to an adjacent array of non-specular scales (orange and red lines). Faded lines represent individual measurements within the same wing surface. Dotted lines indicate the averaged spectra of polished aluminum foil for comparison. **(D–G,I,K)** High-magnification reflected-light microscopy of single metallic scales using a MPlanFLN 50× lens **(D–F)**, and an LMPlan Achromatic 100× lens **(G,I,K)**. **(H,J,L)** SEM top views of metallic scales. **(M–O)** SEM of transversal sections. In *A. formosus* **(O)**, more proximal regions of the scale (dark gray, upper) have thicker lower laminae than distal regions (light gray, lower). Scale bars, **(D–F)** = 20 μm; **(G,I,K)** = 10 μm, **(H,J,L,M–O)** = 1 μm.

mode of additive color mixing. Some of this color gradient is hinted at in our spectral measurements, which exhibited a pronounced peak in the long wavelengths due to the fact that the light paths of the MSP instrument are coaxial and normal to the wing surface, and thus likely to measure the apex and orange-red portion of the scale.

The external aspect of the *H. apelles* upper surface is also peculiar, with large inter-ridge distances (**Figure 3B**) and periodic

crossribs that are perfectly perpendicular to the ridges, indicative of the complete flatness of the upper lamina (**Figure 6J**). The internal anatomy of cross-sectioned scales also revealed a divergent morphology, lacking the marks of transversal periodicity observed in undulatory thin-film types. Instead, the upper lamina and its underlying air layer are flat, and the ridges appear as thin vertical walls that are unlikely to provide sufficient light diffraction for producing dense arrays of colors. Another anatomical feature that varies in the longitudinal axis must thus explain the proximo-distal color gradient. Interestingly, the lower lamina shows a double-layering reminiscent of the Type-IIa multilayered thin films observed in other iridescent lycaenids (Lippert and Gentil, 1959; Schmidt and Paulus, 1970; Tilley et al., 2002; Biró et al., 2007) and in sunset moths (Prum et al., 2006; Yoshioka and Kinoshita, 2007; Yoshioka et al., 2008). To suggest an optical mixing for the observed color mixing, we sought to examine if thickness and periodicity parameters of this system varied in the longitudinal direction. Unfortunately, the fragility of those scales prevented us from properly cryo-fracturing those scales and imaging them in the sagittal plane with SEM. Thus, further characterization of this newly discovered broadband reflector will require alternative methods such as transmission electron microscopy (TEM), identification of the parameters that vary in the proximo-distal axis, and proper biophysical modeling.

A Simple Lower Lamina Thickness Likely Drives Gold Reflectance in a Riodinid

We further examined the gold scales of a riodinid, *A. formosus*. Microspectrophotometry shows remarkable brightness in the 500–800 nm green-to-infrared range (**Figure 6C**), and a lower reflectance in the UV-to-blue range ($<$ 500nm), consistent with the gold rather than silver sheen of this reflector. Reflected microscopy reveals longitudinal stripes of green, yellow, and red colors, but unlike in the typical undulatory thin-films, we were unable to resolve such transitions across distance of 1–3 μm with a 100× lens (**Figures 6F,K**). The *A. formosus* gold scale upper lamina and inner air layer, as observed in top and cross-sectional views (**Figures 6L,O**), also contradicts the role of an undulatory thin-film as defined above. In the absence of any other obvious optically relevant structures, the lower lamina of those scales is likely responsible for their bright reflectance. This is supported by the fact that in comparison, the subjacent scale fractured at a location ∼10 μm closer to the distal edge displays a significantly thinner lower lamina. Although this change in thickness appears to occur over a small proximo-distal distance, note that the transition from blue-violet to yellow-green color is similarly rapid (**Figure 6O**). Indeed, according to thin-film models that incorporate the refractive index of chitin, thicker laminae reflect shorter wavelengths (Stavenga et al., 2014). We thus expect the violet/blue base of the *A. formosus* scale to be thicker than the rest of the scale, which only shows green-yellow-red colors under the reflected light microscope (**Figures 6F,K**), and the green-to-infrared shifts responsible for the spectrally broad gold likely arise from microvariations in lower lamina thickness that we could not detect with SEM. Overall, these results suggest that the bright gold iridescence of the riodinid *A. formosus* scales derives from

a relatively simple reflector with a flat upper lamina and lumen, and a variable lower lamina. In contrast with the nymphalid butterflies that use lower laminae to reflect homogenous color spectra (Stavenga et al., 2014; Wasik et al., 2014; Thayer et al., 2020), we infer that local heterogeneities in those structures may underlie the spectral spread and spatial mixing of reflected colors in the green-to-red range.
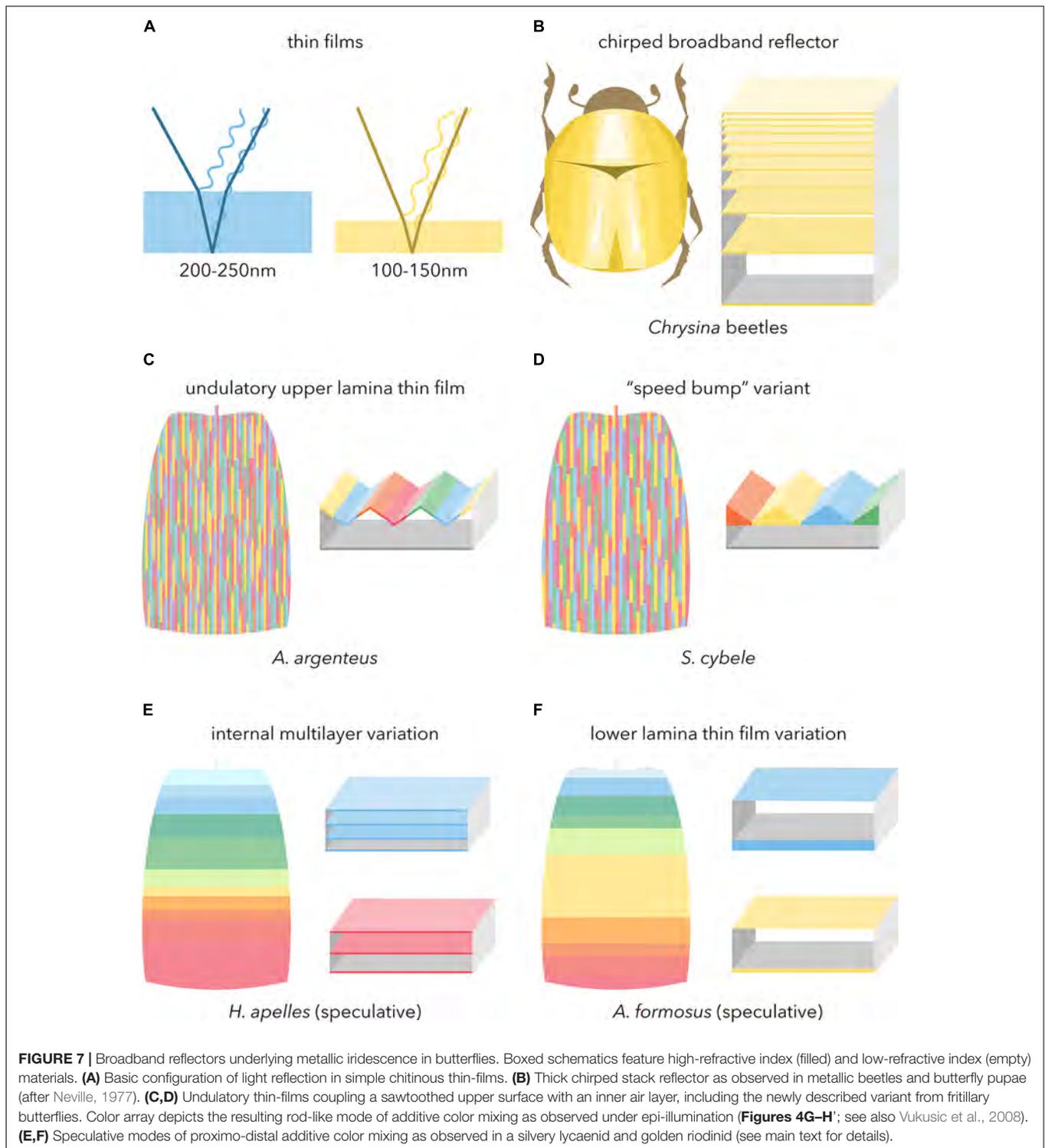
DISCUSSION

Metallic Coloration in Lepidoptera

We compared optical and ultrastructural structural aspects of metallic scales in five out of seven families of Papilionoidea (*sensu* Espeland et al., 2018), and identified several types of broadband reflectors that use distinct chitinous modifications to achieve additive color mixing, including two modes of metallic coloration that remain speculative before further biophysical characterization (**Figure 7**). While our phylogenetic sampling is currently too coarse for ancestral state reconstruction or detailed retracing of the evolution of metallic colorations on the butterfly phylogeny, we are starting to uncover general patterns of phenotypic convergence where sometimes similar, and sometimes novel ultrastructures achieve specular, broad-spectrum reflectance. Beyond butterflies, there is also a tremendous diversity of analogous metallic colorations in moths, including in Hepialidae (e.g., *Korscheltellus lupulinus*), Tortricidae (e.g., *Pelochrista ridingsana*), Crambidae (e.g., *Ramila ruficostalis*), Nolidae (e.g., the Mirror Moth *Titulcia confictella*), Cosmopterigidae (e.g., *Cosmopterix montisella*), and Saturniidae (e.g., *Attacus atlas*). In this section, we provide an overview of the different types of broadband reflectors that have evolved in Lepidoptera.

Undulatory Thin-Film Broadband Reflectors

The undulatory thin-film type described in *A. argenteus* is characterized by a continuous upper lamina, and an inner air layer of periodic thickness (Vukusic et al., 2008). This sawtoothed thin-film results in a mode of spatial color mixing where reflected wavelengths alternate across a 1–3 μm interval in the transversal axis. We recovered similar features in two other Nymphalidae, *A. vanillae* and *S. cybele*, with the nuance that the *S. cybele* thin-film showed dome shaped thickenings of the chitin layer at the level of ridges, rather than a sawtooth shaped lumen as observed in *A. vanillae* and our other samples (**Figures 7C,D**). This reinforces the previously made inference that silver patterns are a homoplasy within different "fritillary" butterflies of the subfamily Heliconiinae (Simonsen, 2007), specifically between tribe Argynnini such as *S. cybele*, and basal members of tribe Heliconiini such as *A. vanillae*. Second, Argynnini displays a variety of reflective scales that vary from dull white to shiny silver and that are similar in external ultrastructures (Simonsen, 2007), but likely vary slightly in their transversal geometry. A similar architecture and mode of additive color mixing has been well-described in the noctuid moth *Eudocima materna*, where apposition of mirror scales with pigmented scales yields

FIGURE 7 | Broadband reflectors underlying metallic iridescence in butterflies. Boxed schematics feature high-refractive index (filled) and low-refractive index (empty) materials. **(A)** Basic configuration of light reflection in simple chitinous thin-films. **(B)** Thick chirped stack reflector as observed in metallic beetles and butterfly pupae (after Neville, 1977). **(C,D)** Undulatory thin-films coupling a sawtoothed upper surface with an inner air layer, including the newly described variant from fritillary butterflies. Color array depicts the resulting rod-like mode of additive color mixing as observed under epi-illumination (**Figures 4G–H**'; see also Vukusic et al., 2008). **(E,F)** Speculative modes of proximo-distal additive color mixing as observed in a silvery lycaenid and golden riodinid (see main text for details).

an angle-dependent reflective effect (Kelley et al., 2019). In this framework, specularity may be achieved by efficient angular reflections in the inter-ridge intervals and spatial color mixing, while more dull states could result from profiles that scatter more light. The evolution of undulatory broadband reflectors may proceed by increases in the amplitude of light-scattering thin-films, notably from scales in a full white state where the upper lamina is unperforated. If this holds true in Heliconiinae, then this mode of convergence in silver iridescence may extend to Satyrinae (Vukusic et al., 2008; García-Barros and Meneguz, 2012), and other butterfly families as we documented here in Hesperiidae, Pieridae, and one out of our two Lycaenidae samples

(*C. lohita*). In any case, the hollow lepidopteran *bauplan* scale type (Ghiradella, 2010) that is necessary to yield the undulatory thin-film seemingly extends to some early diverging branches of the lepidopteran phylogeny (Simonsen, 2001). We predict that the most distant case of convergent undulatory thin-film may have occurred in silver-reflective Hepialidae such as the silver-spotted ghost moth (*Leto venus*), since reflective white scales in this family show a bilayered architecture reminiscent of the butterflies and skippers studied here (Simonsen, 2002).

Proximo-Distal Color Mixing in the Multilayered Scales of Lycaenids

We discovered a new mode of broad-reflectance in *H. apelles* where the visible color spectrum is selectively reflected across the proximo-distal axis of the scale, from violet and blue colors at the base, to red at the tip (**Figures 6E,I**). This rainbow transition in the near field, likely coupled to scale stacking, produces broadband reflectance in the far field. What can we infer about the ultrastructural basis of this proximodistal color mixing? In *H. apelles*, the multilayered lower lamina (**Figure 6N**) is reminiscent of body-lamellae scale iridescence that are widespread in Lycaenidae (Lippert and Gentil, 1959; Schmidt and Paulus, 1970; Tilley et al., 2002; Biró et al., 2007; Wilts et al., 2008). In those butterflies, additional chitin layers increase reflectance, meaning that the multilayered lower lamina contributes to the brightness of the scales (Wilts et al., 2008). Sunset moths also show analogously multilayered structures, and changes in the thickness and spacing of their internal layers on the order of 10–50 nm are responsible for shifts as drastic as pale blue to orange (Yoshioka and Kinoshita, 2007; Yoshioka et al., 2008, 2013; Imafuku et al., 2012). In addition, melanin is present in the distal portion of the scale and absent at the base, perhaps increasing chitin refractive index or even forming a gradient that could contribute to spectral spread (Land, 1972). While we could not resolve here the mechanisms responsible for the continuous color transition from blue to red hues, we extrapolate that microvariations in layering and refractivity drive this shift along single scales (**Figure 7E**).

From an evolutionary perspective, one may postulate that the multilayered state of lycaenid and other body-lamellae ("Type IIa") color iridescent scales (Ghiradella, 1989; Vukusic et al., 2000; Mouchet and Vukusic, 2018) can prime the evolution of broadband reflectance. In *Hypochrysops spp.*, the iridescent blue scales widespread across the dorsal surface are composed of a lower lamina of 7–8 layers and a perforated upper lamina (Ingram and Parker, 2008) while we have observed three layers in the ventral silver scales. Transition to the silver state would then require a filling of the perforations in the upper lamina, and merging of internal layers to produce a variety of chitin layer thicknesses and spacings along the proximo-distal axis.

Tuning of Lower Lamina in the Gold Scales of a Riodinid

The optical and structural basis of color mixing in the specular scales of metalmarks butterflies (Riodinidae) has remained undescribed, and our data from the gold scales of *A. formosus*

showed an original configuration. These were the brightest among all the species sampled here, but their ultrastructure simply consisted of a flat, mostly featureless upper lamina, a flat air lumen, and a similarly flat lower lamina. We propose that a rapid and pronounced reduction in lower lamina thickness is responsible for the abrupt shift from blue-violet to yellow-green in the most proximal third of the scale. This thick (200–250 nm) region appearing blue is consistent with models and existing examples of thin-films (Stavenga et al., 2014; Thayer et al., 2020), and likewise a drop to 100–150 nm produces red and yellow (Thayer et al., 2020). We extrapolate then that microvariations in lower lamina thickness are likely responsible for the reds, yellows, and greens in the majority of the scale (**Figure 7F**), but we were unable to generate interpretable sagittal sections by cryofracture due to scale fragility. Most intriguing, it remains unclear how *A. formosus* achieved brightness levels that exceeded the reflectance of our specular reflectance standard (measurements > 1.00 in **Figure 6C**), a level of gold iridescence that is only achieved in other insects with much thicker stacks of chitin (Steinbrecht et al., 1985; Seago et al., 2009; Biro and Vigneron, 2011). While we have described here the "metalmark" (riodinid) system superficially, a better understanding of how such seemingly flat, simple, and ultrathin sandwich of chitin and air can yield an intensely specular output will be of particular interest.

Broadband Microrib Gratings

A fourth type of metallic reflectance mechanism has been described in the literature, but was not observed in this study. We dub "microrib grating" a type of 2D diffraction grating made of dense herringbone crossrib arrays, and where upper and lower laminae are apposed ("fused scales"), forming a single thin film without a lumen. It has been linked to silver/gold iridescence in the skipper butterfly *Carystoides escalantei* (Ge et al., 2017). Outside of the butterfly/skipper lineage, it has been best characterized in the Micropterigidae *Micropterix calthella* (Kilchoer et al., 2019), where the fused lamina acts as a bronze/gold thin-film reflector whose specularity is enhanced by the diffractive scattering of the overlaying microribs (D'Alba et al., 2019). Other likely examples include the Noctuidae moths *Diachrysia (Plusia) balluca* and *Trichoplusia orichalcea* (Ghiradella, 1991; Brink et al., 1995). Scales from *Adela reaumurella* (Adelidae) and *Stigmella malella* (Nepticulidae) show fused laminae and herringbone microribs that are consistent with the metallic sheens of these moths (van Eldijk et al., 2018). The white reflective scales of *Paysandisia archon* (Castniidae) display this arrangement (Stavenga et al., 2018). In Papilionidae, the reflective component of the glass scales of *G. sarpedon* is also due to a microrib grating, with membranal bilin pigments restricting the reflectance spectrum to a blue-green hue (Stavenga et al., 2010, 2012). In the basal Papilionidae *Baronia brevicornis*, an electron micrograph also suggests a microrib grating arrangement that is indicative of a reflective type (Simonsen et al., 2011), but it is unclear if the image was taken from a silver morph of this polymorphic species (Vazquez, 1987). Herringbone patterns and fused laminae are characteristic of early diverging lepidopteran lineages (Kristensen, 1970;

Simonsen, 2001; Deparis et al., 2006) and in accordance with these authors, we extrapolate that the microrib diffraction grating could be a sophistication of the lepidopteran scale ancestral state, but it is also noteworthy that a convergent scale morphology and microrib grating mechanism have been linked to gold iridescence in Collembola, suggesting the optical trick may extend across many hexapod lineages that also bear cuticular scales (D'Alba et al., 2019). In any case, we gather from the literature that diffraction gratings consisting of dense microribs and apposed laminae are likely common and ancient enhancers of metallic coloration in Lepidoptera.

CONCLUSION

Metallic appearances require spectral spread that result from increased reflectance variance in the geometry of the scale thin-films. The literature has pinpointed 2D diffraction gratings, characterized by dense herringbone microribs and apposed lower laminae, as a common theme for metallic reflections. Our study indicates that in butterflies and beyond, a bright output requires an unperforated upper lamina, and that broadband reflectance is also often reached by transversal undulations of the upper chitinous section and air lumen (**Figures 7D–G**). This configuration may be a simple derivation from traditional scale types including depigmented, white light-scattering scales. Proximo-distal thickness gradients in the lower section of the scale (simple or multilayered lower laminas) appear as another mode of broadband reflectance as alluded in Lycaenidae and Riodinidae, a phenomenon that will require further comparative studies and biophysical characterization.

MATERIALS AND METHODS

Butterflies

A. vanillae larvae were obtained from Shady Oak Farms (Florida, United States) and reared on *Passiflora suberosa* or *Passiflora incarnata* until adult emergence. Specimens of *S. cybele*, *C. eurytheme*, *Z. cesonia*, and *E. clarus* were collected from wild populations in the vicinity of Silver Spring (Maryland, United States), Mason Neck (Virginia, United States), Starkville (Mississippi, United States), and Washington (District of Columbia, United States), respectively. Specimens of *H. apelles* (*orig.* Papua – New Guinea), *C. (Spindasis) lohita* (*orig.* Bali, Indonesia), and *A. formosus* (*orig.* Peru) were imported from online retailers with appropriate collection and transit permits.

Color and UV Macro-Photography

Pinned specimens were imaged in the visible range using a Nikon D5300 camera mounted with a Micro-Nikkor 105mm f/2.8G lens on a StackShot rail and focused-stacked using the Helicon Remote and Helicon Focus software. A Keyence VHX-5000 digital microscope was used to generate stitched high-resolution images of wing patterns using a VH-Z00T lens at 50× magnification and a VH-Z100T lens at the 300× magnification. UV-photography was performed under the illumination of GE BlackLight 13-Watt T3 Spiral Light Bulbs, using a full-spectrum converted Panasonic G3 camera, mounted with a Kyoei-Kuribayashi 35mm F3.5 lens on a helicoid focusing adapter, and stacked Hoya U-330 and Schott BG39 1.5 mm glass filters eliminating the visible and infrared wavelengths above 400 nm.

Single-Scale Light Microscopy

Individual scales were removed from spread butterflies and positioned on a glass slide with an eyelash tool, and stitch-imaged with a Keyence VHX-5000 microscope in reflected light mode and a VH-Z100R lens at 1000× magnification. All scales were imaged in full coaxial lighting except for *H. apelles*, which required additional ring lighting for best balance of resolution and color features. The same scales were then immersed in clove oil, mounted with a coverslip, and imaged in transmission mode. For reflective microscopy, single scales were imaged with an Olympus BX53M microscope in Reflected Bright-Field mode, mounted with an Olympus MPlanFLN 50×/NA 0.80 objective and an SC50 color camera, before focus-stacking with the Olympus Stream software, and XY-stitching in Adobe Photoshop. For reflective microscopy at higher-magnifications, the same scales were imaged on a trinocular AmScope ME580-2L metallurgical microscope mounted with a Nikon D5300 camera, a Varimag II camera adapter at 3.5× magnification setting, and an LMPlan Achromatic 100×/NA 0.8 long working distance objective. Optimal balance of resolution and color features were obtained under polarized light with a field diaphragm at maximal shutting position, and an aperture diaphragm on 60–80% shut position.

Spectral Measurements

Reflectance spectra were measured from a 250 μm^2 region of the surface of intact wing sections, and thus represent the combined reflectance of cover scales, underlying ground scales, and wing membrane (Stavenga et al., 2014). Reflectance measurements were taken using a custom-built microspectrophotometer (20/20PV, CRAIC Technologies, Inc., San Dimas, CA, United States) equipped with a 5× UV-vis objective (LMU-5X-NUV, Thorlabs, Inc., Newton, NJ, United States). Samples were illuminated with a xenon arc lamp (XBO 75 W/2, OSRAM GmbH, Munich, Germany), with the light path oriented normal to the wing surface and coaxial with the axis of light collection. Reflectance spectra were calculated in relation to a high-reflectivity specular reflectance standard (STAN-SSH-NIST, Ocean Optics, Inc., Dunedin, FL, United States). For each scale type, individual spectra were the average of 25 spectra measured consecutively (integration time: 200–350 ms, total measurement time per average spectra: 5–8.75 s). In order to provide a familiar point of comparison, measurements were also taken on the polished and dull side of aluminum foil (0.018 mm, Fisherbrand), and resulted in spectra consistent with other studies (Vukusic et al., 2008; Pozzobon et al., 2020).

Scanning Electron Microscopy (SEM)

For surface imaging of scales of distinct identities, wing patterns of interest were excised and mounted on SEM stubs with double-sided carbon tape, and color imaged under the Keyence VHX-5000 microscope for registration of scale type. Samples were sputter-coated with two 12.5 nm layers of gold for improving sample conductivity, with the second layer applied after tilting the stub by 45°. SEM images were acquired on a FEI Teneo LV SEM, using secondary electrons (SE) and an Everhart-Thornley detector (ETD) using a beam energy of 2.00 kV, beam current of 25 pA, and a 10 μs dwell time. Individual images were stitched using the Maps 3.10 software (Thermo Fisher Scientific).

To minimize charging for high magnification views of scale surface morphology, individual scales were collected by brushing the surface of the wing with an eyelash tool, then dusted onto an SEM stub with double-sided carbon tape. Stubs were sputter-coated with one 12.5 nm layer of gold, and imaged at 2.00 kV/25 pA with a 10 μs dwell time. One sample per species was imaged, and all the SEM images used for morphometric analysis are accessible on the Dryad online repository (Day et al., 2020).

For documenting internal scale anatomy, silver pattern elements were excised and cryo-fractured following previous recommendations (Wasik et al., 2014; Matsuoka and Monteiro, 2018; Thayer et al., 2020). Briefly, wing sections were submerged in liquid nitrogen, immediately placed silver-side down onto a silicon wafer, and cut with a fresh ceramic-coated microtome blade. Alternatively, excised wing sections were placed silver-side down onto a silicon wafer and secured with foam board, glassine, and a binder clip before submersion in liquid nitrogen and cutting as previously described. After allowing to dry, individual cut scales were placed using an eyelash tool on copper tape, such that the cut edges were approximately parallel to and overhanging the tape edge. The copper tape was bent to 90° and placed on a stub so that the scales' cut edges faced upwards, i.e., normal to the stub surface, and secured with additional copper tape. The stubs were sputter-coated with a 10–12.5 nm layer of gold, and imaged at 5.00 kV/6.3 pA and a 10 μs dwell time.

Morphometric Analysis

Morphometric measurements of scale widths and ridge distances were carried out on 25 scales of each color from eight species, using a custom semi-automated R pipeline that derives ultrastructural parameters from large SEM images (Day et al., 2019). Briefly, ridge spacing was assessed by Fourier transforming intensity traces of the ridges acquired from the FIJI software (Schindelin et al., 2012). Scale width was directly measured in FIJI by manually tracing a line, orthogonal to the ridges, at the section of maximal width.

DATA AVAILABILITY STATEMENT

The datasets generated for this study are available on request to the corresponding author.

AUTHOR CONTRIBUTIONS

AR and CD equally performed all the imaging and experiments, and contributed to the figures and data analysis. JH, BC, and NM contributed to the data analysis and intellectual support. AM supervised the project and wrote the manuscript with input from all co-authors. All authors contributed to the article and approved the submitted version.

FUNDING

ACKNOWLEDGMENTS

REFERENCES

Agez, G., Bayon, C., and Mitov, M. (2017). Multiwavelength micromirrors in the cuticle of scarab beetle *Chrysina gloriosa*. *Acta Biomater.* 48, 357–367. doi: 10.1016/j.actbio.2016.11.033

Berthier, S. (2007). *Iridescences: The Physical Colors Of Insects*. Berlin: Springer.

Biró, L. P., Kertész, K., Vértesy, Z., Márk, G. I., Bálint, Z., Lousse, V., et al. (2007). Living photonic crystals: butterfly scales—nanostructure and optical properties. *Mater. Sci. Eng. C* 27, 941–946. doi: 10.1016/j.msec.2006.09.043

Biro, L. P., and Vigneron, J.-P. (2011). Photonic nanoarchitectures in butterflies and beetles: valuable sources for bioinspiration. *Laser Photon. Rev.* 5, 27–51. doi: 10.1002/lpor.200900018

Brink, D. J., Smit, J. E., Lee, M. E., and Möller, A. (1995). Optical diffraction by the microstructure of the wing of a moth. *Appl. Opt.* 34, 6049–6057.

Briscoe, A. D., Bybee, S. M., Bernard, G. D., Yuan, F., Sison-Mangus, M. P., Reed, R. D., et al. (2010). Positive selection of a duplicated UV-sensitive visual pigment coincides with wing pigment evolution in heliconius butterflies. *Proc. Natl. Acad. Sci. U.S.A.* 107, 3628–3633. doi: 10.1073/pnas.0910085107

Chiadini, F., Fiumara, V., and Scaglione, A. (2017). Design of bioinspired chirped reflectors using a genetic algorithm. *Bioinspirat. Biomimet. Bioreplicat.* 2017:101620T.

Cook, C. Q., and Amir, A. (2016). Theory of chirped photonic crystals in biological broadband reflectors. *Optica* 3, 1436–1439.

D'Alba, L., Wang, B., Vanthournout, B., and Shawkey, M. D. (2019). The golden age of arthropods: ancient mechanisms of colour production in body scales. *J. R. Soc. Interf.* 16:20190366.

Day, C. R., Hanly, J. J., Ren, A., and Martin, A. (2019). Sub-micrometer insights into the cytoskeletal dynamics and ultrastructural diversity of butterfly wing scales. *Dev. Dyn.* 248, 657–670. doi: 10.1002/dvdy.63

Day, C. R., Hanly, J. J., Ren, A., and Martin, A. (2020). *Data from: Convergent Evolution of Broadband Reflectors Underlies Metallic Colorations*

in Butterflies, v3, Dryad, Dataset. Available online at: https://doi.org/10.5061/dryad.2fqz612mc

Denton, E. J., and Land, M. F. (1971). Mechanism of reflexion in silvery layers of fish and cephalopods. *Proc. R. Soc. Lond. Ser. B Biol. Sci.* 178, 43–61. doi: 10.1098/rspb.1971.0051

Deparis, O., Vandenbem, C., Rassart, M., Welch, V. L., and Vigneron, J.-P. (2006). Color-selecting reflectors inspired from biological periodic multilayer structures. *Optics Exp.* 14, 3547–3555.

Dinwiddie, A., Null, R., Pizzano, M., Chuong, L., Krup, A. L., Tan, H. E., et al. (2014). Dynamics of F-actin prefigure the structure of butterfly wing scales. *Dev. Biol.* 392, 404–418. doi: 10.1016/j.ydbio.2014.06.005

Dolan, J. A., Wilts, B. D., Vignolini, S., Baumberg, J. J., Steiner, U., and Wilkinson, T. D. (2015). Optical properties of gyroid structured materials: from photonic crystals to metamaterials. *Adv. Opt. Mater.* 3, 12–32. doi: 10.1002/adom.201400333

Espeland, M., Breinholt, J., Willmott, K. R., Warren, A. D., Vila, R., Toussaint, E. F., et al. (2018). A comprehensive and dated phylogenomic analysis of butterflies. *Curr. Biol.* 28, 770–778.

García-Barros, E., and Meneguz, M. (2012). Estructura de las escamas ventrales de las alas de *Coenonympha Hübner*,[1819], con especial referencia a *C. pamphilus* (L., 1758) y su morfotipo lyllus (Esper, 1805)(Lepidoptera: Nymphalidae). *SHILAP Rev. Lepidopterol.* 40, 279–293.

Ge, D., Wu, G., Yang, L., Kim, H.-N., Hallwachs, W., Burns, J. M., et al. (2017). Varying and unchanging whiteness on the wings of dusk-active and shade-inhabiting *Carystoides escalantei* butterflies. *Proc. Natl. Acad. Sci. U.S.A.* 114, 7379–7384. doi: 10.1073/pnas.1701017114

Ghiradella, H. (1989). Structure and development of iridescent butterfly scales: lattices and laminae. *J. Morphol.* 202, 69–88. doi: 10.1002/jmor.1052020106

Ghiradella, H. (1991). Light and color on the wing: structural colors in butterflies and moths. *Appl. Opt.* 30, 3492–3500.

Ghiradella, H. (2010). Insect cuticular surface modifications: scales and other structural formations. *Adv. Insect Physiol.* 38, 135–180. doi: 10.1016/s0065-2806(10)38006-4

Ghoshal, A., DeMartini, D. G., Eck, E., and Morse, D. E. (2013). Optical parameters of the tunable Bragg reflectors in squid. *J. R. Soc. Interf.* 10:20130386. doi: 10.1098/rsif.2013.0386

Giraldo, M. A. (2008). *Butterfly Wing Scales: Pigmentation and Structural Properties.* Thesis, University of Groningen. doi: 10.1098/rsif.2013.0386

Holt, A. L., Sweeney, A. M., Johnsen, S., and Morse, D. E. (2011). A highly distributed Bragg stack with unique geometry provides effective camouflage for Loliginid squid eyes. *J. R. Soc. Interf.* 8, 1386–1399. doi: 10.1098/rsif.2010.0702

Imafuku, M., Kubota, H. Y., and Inouye, K. (2012). Wing colors based on arrangement of the multilayer structure of wing scales in lycaenid butterflies (Insecta: Lepidoptera). *Entomol. Sci.* 15, 400–407. doi: 10.1111/j.1479-8298.2012.00525.x

Ingram, A. L., and Parker, A. R. (2008). A review of the diversity and evolution of photonic structures in butterflies, incorporating the work of John Huxley (The Natural History Museum, London from 1961 to 1990). *Philos. Trans. R. Soc. B Biol. Sci.* 363, 2465–2480. doi: 10.1098/rstb.2007.2258

Jordan, T. M., Partridge, J. C., and Roberts, N. W. (2012). Non-polarizing broadband multilayer reflectors in fish. *Nat. Photon.* 6:759. doi: 10.1038/nphoton.2012.260

Kelley, J. L., Tatarnic, N. J., Schröder-Turk, G. E., Endler, J. A., and Wilts, B. D. (2019). A dynamic optical signal in a nocturnal moth. *Curr. Biol.* 29, 2919–2925.

Kilchoer, C., Steiner, U., and Wilts, B. D. (2019). Thin-film structural coloration from simple fused scales in moths. *J. R. Soc. Interf. Focus* 9:20180044. doi: 10.1098/rsfs.2018.0044

Kinoshita, S. (2008). *Structural Colors In The Realm Of Nature.* Singapore: World Scientific.

Kinoshita, S., and Yoshioka, S. (2005). Structural colors in nature: the role of regularity and irregularity in the structure. *Chemphyschem* 6, 1442–1459. doi: 10.1002/cphc.200500007

Kristensen, N. P. (1970). Morphological observations on the wing scales in some primitive *Lepidoptera* (Insecta). *J. Ultrastruct. Res.* 30, 402–410. doi: 10.1016/s0022-5320(70)80071-5

Land, M. F. (1972). The physics and biology of animal reflectors. *Prog. Biophys. Mol. Biol.* 24, 75–106. doi: 10.1016/0079-6107(72)90004-1

Lee, D. W. (2009). "Plant tissue optics: micro-and nanostructures," in *Proceedings of the Biomimetics and Bioinspiration*, San Diego, CA.

Leertouwer, H. L., Wilts, B. D., and Stavenga, D. G. (2011). Refractive index and dispersion of butterfly chitin and bird keratin measured by polarizing interference microscopy. *Opt. Exp.* 19, 24061–24066.

Levy-Lior, A., Pokroy, B., Levavi-Sivan, B., Leiserowitz, L., Weiner, S., and Addadi, L. (2008). Biogenic guanine crystals from the skin of fish may be designed to enhance light reflectance. *Cryst. Growth Design* 8, 507–511. doi: 10.1021/cg0704753

Lippert, W., and Gentil, K. (1959). Über lamellare feinstrukturen bei den schillerschuppen der schmetterlinge vom urania-und morpho-typ. *Zeitschrift Morphol. Ökol. Tiere* 48, 115–122. doi: 10.1007/bf00407836

Liu, X., Wang, D., Yang, Z., Zhou, H., Zhao, Q., and Fan, T. (2019). Bright silver brilliancy from irregular microstructures in butterfly *Curetis acuta* moore. *Adv. Opt. Mater.* 7:1900687. doi: 10.1002/adom.201900687

Matsuoka, Y., and Monteiro, A. (2018). Melanin pathway genes regulate color and morphology of butterfly wing scales. *Cell Rep.* 24, 56–65. doi: 10.1016/j.celrep.2018.05.092

Mayor, A. G. (1806). *The Development of the Wing Scales and Their Pigment in Butterflies and Moths.* Cambridge, MA: Harvard College.

McKenzie, D. R., Yin, Y., and McFall, W. D. (1995). Silvery fish skin as an example of a chaotic reflector. *Proc. R. Soc. Lond. Ser. A Math. Phys. Sci.* 451, 579–584. doi: 10.1098/rspa.1995.0144

Mouchet, S. R., and Vukusic, P. (2018). Structural colours in lepidopteran scales. *Adv. Insect Physiol.* 54, 1–53. doi: 10.1016/bs.aiip.2017.11.002

Neville, A. C. (1977). Metallic gold and silver colours in some insect cuticles. *J. Insect Physiol.* 23, 1267–1274. doi: 10.1016/0022-1910(77)90069-5

Pozzobon, V., Levasseur, W., Do, K.-V., Palpant, B., and Perré, P. (2020). Household aluminum foil matte and bright side reflectivity measurements: application to a photobioreactor light concentrator design. *Biotechnol. Rep.* 25:e00399. doi: 10.1016/j.btre.2019.e00399

Prum, R. O., Quinn, T., and Torres, R. H. (2006). Anatomically diverse butterfly scales all produce structural colours by coherent scattering. *J. Exp. Biol.* 209, 748–765. doi: 10.1242/jeb.02051

Schindelin, J., Arganda-Carreras, I., Frise, E., Kaynig, V., Longair, M., Pietzsch, T., et al. (2012). Fiji: an open-source platform for biological-image analysis. *Nat. Methods* 9:676. doi: 10.1038/nmeth.2019

Schmidt, K., and Paulus, H. (1970). Die feinstruktur der flügelschuppen einiger *Lycaeniden* (Insecta, Lepidoptera). *Zeitschrift Morphol. Tiere* 66, 224–241. doi: 10.1007/bf00280735

Seago, A. E., Brady, P., Vigneron, J.-P., and Schultz, T. D. (2009). Gold bugs and beyond: a review of iridescence and structural colour mechanisms in beetles (Coleoptera). *J. R. Soc. Interf.* 6, S165–S184.

Simonsen, T. J. (2001). The wing vestiture of the non-ditrysian *Lepidoptera* (Insecta). Comparative morphology and phylogenetic implications. *Acta Zool.* 82, 275–298. doi: 10.1046/j.1463-6395.2001.00089.x

Simonsen, T. J. (2002). Wing scale covering supports close relationship between *Callipielus* and *Dalaca*, austral South American ghost moths (Lepidoptera: Hepialidae). *Stud. Neotrop. Fauna Environ.* 37, 65–69. doi: 10.1076/snfe.37.1.65.2117

Simonsen, T. J. (2007). Comparative morphology and evolutionary aspects of the reflective under wing scale-pattern in Fritillary butterflies (Nymphalidae: Argynnini). *Zool. Anzeiger A J. Compar. Zool.* 246, 1–10. doi: 10.1016/j.jcz.2005.04.005

Simonsen, T. J., Zakharov, E. V., Djernaes, M., Cotton, A. M., Vane-Wright, R. I., and Sperling, F. A. (2011). Phylogenetics and divergence times of *Papilioninae* (Lepidoptera) with special reference to the enigmatic genera Teinopalpus and Meandrusa. *Cladistics* 27, 113–137. doi: 10.1111/j.1096-0031.2010.00326.x

Singer, A., Boucheron, L., Dietze, S. H., Jensen, K. E., Vine, D., McNulty, I., et al. (2016). Domain morphology, boundaries, and topological defects in biophotonic gyroid nanostructures of butterfly wing scales. *Sci. Adv.* 2:e1600149. doi: 10.1126/sciadv.1600149

Stavenga, D. G., Giraldo, M. A., and Leertouwer, H. L. (2010). Butterfly wing colors: glass scales of *Graphium sarpedon* cause polarized iridescence and enhance blue/green pigment coloration of the wing membrane. *J. Exp. Biol.* 213, 1731–1739. doi: 10.1242/jeb.041434

Stavenga, D. G., Leertouwer, H. L., Meglič, A., Drašlar, K., Wehling, M. F., Pirih, P., et al. (2018). Classical lepidopteran wing scale colouration in the giant butterfly-moth *Paysandisia archon*. *PeerJ* 6:e4590. doi: 10.7717/peerj.4590

Stavenga, D. G., Leertouwer, H. L., Osorio, D. C., and Wilts, B. D. (2015a). High refractive index of melanin in shiny occipital feathers of a bird of paradise. *Light Sci. Appl.* 4:e243. doi: 10.1038/lsa.2015.16

Stavenga, D. G., Matsushita, A., and Arikawa, K. (2015b). Combined pigmentary and structural effects tune wing scale coloration to color vision in the swallowtail butterfly *Papilio xuthus*. *Zool. Lett.* 1:14.

Stavenga, D. G., Leertouwer, H. L., and Wilts, B. D. (2014). Coloration principles of nymphaline butterflies–thin films, melanin, ommochromes and wing scale stacking. *J. Exp. Biol.* 217, 2171–2180. doi: 10.1242/jeb.098673

Stavenga, D. G., Matsushita, A., Arikawa, K., Leertouwer, H. L., and Wilts, B. D. (2012). Glass scales on the wing of the swordtail butterfly *Graphium sarpedon* act as thin film polarizing reflectors. *J. Exp. Biol.* 215, 657–662. doi: 10.1242/jeb.066902

Steinbrecht, R. A., Mohren, W., Pulker, H. K., and Schneider, D. (1985). Cuticular interference reflectors in the golden pupae of danaine butterflies. *Proc. R. Soc. Lond. Ser. B Biol. Sci.* 226, 367–390. doi: 10.1098/rspb.1985.0100

Thayer, R. C., Allen, F. I., and Patel, N. H. (2020). Structural color in Junonia butterflies evolves by tuning scale lamina thickness. *eLife* 9:e52187.

Tilley, R. J. D., Eliot, J. N., and Yoshimoto, H. (2002). Scale microstructure and its phylogenetic implications in lycaenid butterflies (Lepidoptera, Lycaenidae). *Lepidoptera Sci.* 53, 153–180.

van Eldijk, T. J., Wappler, T., Strother, P. K., van der Weijst, C. M., Rajaei, H., Visscher, H., et al. (2018). A Triassic-Jurassic window into the evolution of Lepidoptera. *Sci. Adv.* 4:e1701568. doi: 10.1126/sciadv.1701568

Vazquez, L. G. (1987). *Baronia Brevicornis Salvin Y Sus Formas (Lepidoptera: Papilionidae-Baroniinae)*. México: National Autonomous University of Mexico.

Vukusic, P., Kelly, R., and Hooper, I. (2008). A biological sub-micron thickness optical broadband reflector characterized using both light and microwaves. *J. R. Soc. Interf.* 6, S193–S201.

Vukusic, P., Sambles, J. R., and Ghiradella, H. (2000). Optical classification of microstructure in butterfly wing–scales. *Photon. Sci. News* 6, 61–66.

Wasik, B. R., Liew, S. F., Lilien, D. A., Dinwiddie, A. J., Noh, H., Cao, H., et al. (2014). Artificial selection for structural color on butterfly wings and comparison with natural evolution. *Proc. Natl. Acad. Sci. U.S.A.* 111, 12109–12114. doi: 10.1073/pnas.1402770111

Wiemers, M., Chazot, N., Wheat, C. W., Schweiger, O., and Wahlberg, N. (2019). A complete time-calibrated multi-gene phylogeny of the European butterflies. *bioRxiv* [Preprint]. doi: 10.1101/844175

Wilts, B. D., Leertouwer, H. L., and Stavenga, D. G. (2008). Imaging scatterometry and microspectrophotometry of lycaenid butterfly wing scales with perforated multilayers. *J. R. Soc. Interf.* 6, S185–S192.

Wilts, B. D., Pirih, P., Arikawa, K., and Stavenga, D. G. (2013). Shiny wing scales cause spec (tac) ular camouflage of the angled sunbeam butterfly, *Curetis acuta*. *Biol. J. Linnean Soc.* 109, 279–289. doi: 10.1111/bij.12070

Wilts, B. D., Zubiri, B. A., Klatt, M. A., Butz, B., Fischer, M. G., Kelly, S. T., et al. (2017). Butterfly gyroid nanostructures as a time-frozen glimpse of intracellular membrane development. *Sci. Adv.* 3:e1603119. doi: 10.1126/sciadv.1603119

Yoshioka, S., and Kinoshita, S. (2007). Polarization-sensitive color mixing in the wing of the Madagascan sunset moth. *Opt. Exp.* 15, 2691–2701.

Yoshioka, S., Nakano, T., Nozue, Y., and Kinoshita, S. (2008). Coloration using higher order optical interference in the wing pattern of the Madagascan sunset moth. *J. R. Soc. Interf.* 5, 457–464. doi: 10.1098/rsif.2007.1268

Yoshioka, S., Shimizu, Y., Kinoshita, S., and Matsuhana, B. (2013). Structural color of a lycaenid butterfly: analysis of an aperiodic multilayer structure. *Bioinspirat. Biomimet.* 8:045001.

Zhang, Y., Hayashi, T., Hosokawa, M., Yazawa, S., and Li, Y. (2009). Metallic lustre and the optical mechanism generated from the leaf surface of Begonia rex Putz. *Sci. Hortic.* 121, 213–217. doi: 10.1016/j.scienta.2009.01.030